Pattern Formation in Lepidopteran Wings

Two different kinds of patterns have been studied in lepidopteran wings – *color pattern and the spacing pattern of scale cells*. These patterns exist on two different spatial scales. In the early stages of adult development, precursors of scale cells differentiate throughout each epithelial monolayer and migrate into rows that are roughly parallel to the body axis and regularly spaced about 50 μm apart. We develop a mathematical model for the formation of these parallel rows of scale cells in the developing adult wings of Lepidoptera. We show that the inclusion of biologically realistic adhesive properties of cells, as specified by their positions, is sufficient to generate in a robust manner a series of scale rows along the length of the wing in the correct orientation. We next look briefly at the biology of color pattern formation, and we review some mathematical models for this phenomenon, which, in contrast to the spatial arrangement of scale cells, involves interactions among cells that operate over longer distances.

Key Words: *biological pattern formation, arrangement pattern of scale cells, color pattern, lepidopteran wings*

1 INTRODUCTION

Lepidopteran wing markings are among the most colorful examples of pattern formation in nature. Thousands of scale cells cover moth and butterfly wings in highly ordered and intricate patterns, and individual scale cells can be easily seen through a simple magnifying glass. Two different kinds of patterns are associated with these scales – *color pattern and the spatial arrangement of scale cells*. Color patterns have attracted the interest of taxonomists and developmental biologists for decades and have also provided some of the most dramatic examples of morphological

Comments Theor. Biol.
1998, Vol. 5, No. 2-4, pp. 69–87
Reprints available directly from the publisher
Photocopying permitted by license only

diversity. The colors on wings are imparted by the colors of scale cells that cover the entire wing. The color of scale cells can be due to the presence of chemical pigments,[1] or it is sometimes due to structural colors that arise from the interaction of light beams with the surfaces of the intricately sculptured scales.[2] The color patterns of wings are, in general, finely-tiled mosaic patterns produced by overlapping, monochromatic scales and are characteristic of each lepidopteran species. On the other hand, the arrangements of scale cells do not show species-specific patterns, but they are, in general, common to all lepidopteran wings. The arrangement of scale cells has a number of notable characteristics. Firstly, precursors of scale cells in the developing adult wings rearrange to form nearly parallel rows along the anteroposterior axis of the wing that are maintained throughout and after adult development. Secondly, these rows are arranged at regular spatial intervals along the proximodistal axis. Thirdly, these rows are continuous across the veins in the wing, and they are also continuous around the dorsal and ventral monolayers of the wing. The color patterns of wings are in turn formed by the colors of these regularly-arranged scale cells within each monolayer.

Between pupation and the beginning of adult development, the epithelial cells of the wing are undifferentiated and morphologically homogeneous. About one to three days after pupation (the time depends on the insect and the temperature at which it develops), epithelial cells retract from the pupal cuticle and begin the cell divisions, movements, and morphological differentiation associated with adult development. At this time two cell types can be readily distinguished. The smaller cells are generalized epithelial cells (GECs) of the wing, and the larger cells are scale precursor cells (SPCs) that differentiate from GECs at the inception of adult development. SPCs are arranged in space such that they are separated from each other at regular intervals by GECs. Within a few hours of differentiation of the isotropically-arranged SPCs, these cells become polarized along the proximodistal axis of the wing and begin to align into rows parallel to the anteroposterior axis of the wing. This row formation continues until a stable spatial perodicity of rows is established (Figure 1). These parallel rows of SPCs that are established at the beginning of adult development maintain their arrangement throughout adult development and represent the same rows of scales that appear on the surface of the adult wing.[3,4] The density of SPCs increases during the period of cell rearrangement in the developing adult wing, while the total number of cells in the wing remains almost constant during cell rearrangement.

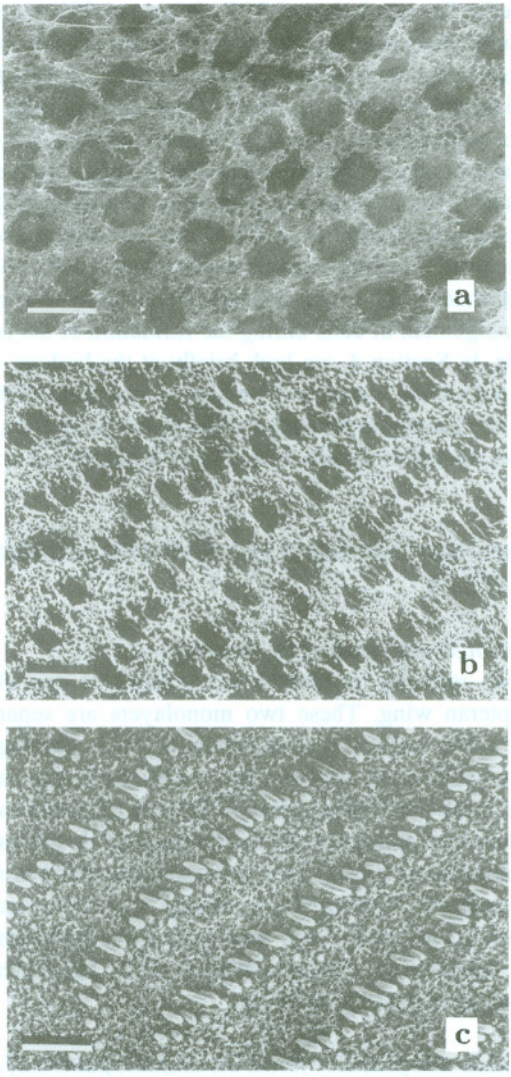

FIGURE 1 Surface views of the dorsal epithelial monolayer of the moth *Manduca* wing at various times after retraction of the epithelial cells from the pupal cuticle. Proximal → distal = upper left → lower right; anterior → posterior = upper right → lower left. (a) At the time of epithelial retraction from the pupal cuticle (2.5 days after pupation), primordial scale cells (dark, circular areas) are distributed in an apparently irregular pattern within the epithelial sheet. The cells have no obvious polarity. (b) Primordial scale cells begin to align in anastomosing rows that lie parallel to the anterior-posterior axis of the wing (3.5 days after pupation). (c) Once the alignment of cells is completed (5 days after pupation), scale cells begin their outgrowth in a proximal to distal direction. A stable periodicity of rows has been established (from Ref. 4 with permission, bar = 50 μm).

The increase in the population of SPCs is around 20% of the total cell population with the exact value depending on the particular insect.[5–7]

The spatial arrangement of scale cells in periodic rows has traditionally not attracted the attention that the study of lepidopteran color patterns has received. Recently, however, progress in understanding the cellular and molecular basis of pattern formation has encouraged a fresh examination of processes involved in generating biological periodicity.[8] In the next section, we summarize what is known about the cellular and molecular processes involved in parallel row formation. In Section 3, we develop a mathematical model with origin-dependent adhesivity to account for the orderly rearrangement of cells during the formation of the parallel rows of scale cells. In Section 4, we look briefly at the biology of the color pattern in lepidopteran wings, and we also review mathematical models for color pattern formation presented so far. In the last section, we discuss general issues related to pattern formation in lepidopteran wings.

2 MECHANISMS FOR PARALLEL ROW FORMATION OF SCALE CELLS

(1) Cell rearrangement occurs in a monolayer

There are two monolayers (dorsal and ventral) of epithelial cells in each lepidopteran wing. These two monolayers are separated by an extracellular space, and cell rearrangement in the developing adult wing has been assumed to occur autonomously within each monolayer without influence from the other monolayer[7,9] (Figure 2). Only during a brief period of adult development in the moth *Manduca* do the basal laminae of the two monolayers break down and transiently form contacts along their basal surfaces. These findings suggest that the process of scale row formation in the lepidopteran wing does not involve complex three-dimensional interactions among epithelial cells, but instead involves simpler two-dimensional interactions.

(2) Lateral inhibition probably forms the uniform pattern of SPCs

Extrapolating from what is known about the generation of patterns in the integument (epithelial cells and the cuticle secreted by these cells) of *Drosophila*, it is possible to envisage how the regular spacing patterns of SPCs are initially established in lepidopteran wings. The initial isotropic spacing of SPCs is strongly suggestive of patterns generated by cells

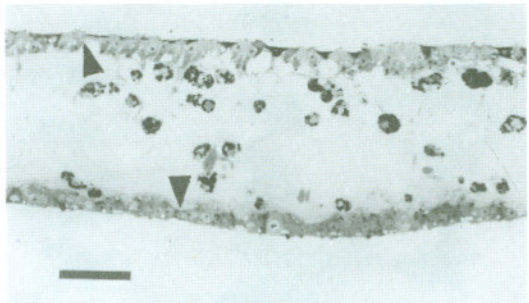

FIGURE 2 The dorsal and ventral monolayers of a moth wing 4 days after pupation. Each monolayer is attached to a convoluted basal lamina (arrowheads). A large extracellular space containing hemocytes separates the two monolayers (from Ref. 4 with permission, bar = 50 μm).

of the *Drosophila* integument. Bristles represent the structures of the fly integument that are developmentally equivalent to the scales of lepidopteran wings. Genetic analysis of regular bristle patterns in the integument of *Drosophila* has revealed most of what we know about the process of generating these spatial patterns of the integument.[10–13] Bristle patterns arise in a stepwise fashion. First a general area is specified in which all cells in the area have the competence to become bristle precursors and then one of these several competent cells is specified to be a bristle precursor cell. Genes of the achaete-scute complex as well as trans-acting regulators of the complex are involved in specifying the group of equivalent cells from which only one cell will be singled out to become a bristle precursor. This cell then inhibits all nearby cells of the equivalence group from realizing their bristle cell potentialities by a process referred to as lateral inhibition.[14,15,5,16] The inhibitory signal emanates from the bristle precursor cell. What molecule(s) make up the inhibitory signal is still a mystery, but several loci are known to be required for transmission of the signal. Two of these loci (*Notch* and *Delta*) encode cell surface proteins and probably mediate lateral inhibition via cell contacts.

(3) Long-range interaction mediated by basal processes

Scanning electron microscopy has been used to visualize the movement of the distinctive SPCs at the surface of the wing monolayer. At the same time, staining of individual cells within the monolayer of coherent cells

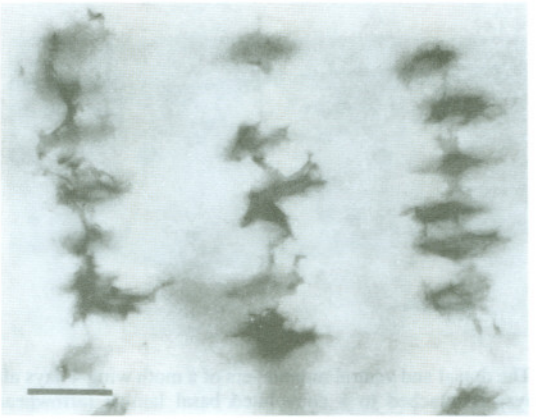

FIGURE 3 In some areas of the wing, only primordial scale cells stain. On day 4 after pupation these cells have begun to align in rows that are regularly spaced along the proximodistal axis. Several basal processes can extend from a given cell. No preferential orientation of processes is evident; they extend along transverse rows as well as between rows (from Ref. 4 with permission, bar = 25 μm).

has allowed the first detailed visualization of cellular events beneath the surface of the monolayer.[4,17] The processes of an individual cell can be traced to reveal the complexity of its interactions with surrounding cells. As the alignment of SPCs into rows proceeds, extension of processes from the basal surfaces of the epithelial cells simultaneously occurs. These processes can extend for distances of several cell diameters and can establish contacts not only with adjacent cells but with cells that are four or five cell diameters away (Figure 3). The extension of basal processes is coincident with the surface rearrangement of cells; as soon as the SPCs have assumed their final positions in the wing monolayer and have begun to extend their polarized scale processes, all cells within the monolayer retract their basal processes. These complex interactions that occur at cell surfaces as cells rearrange and extend basal processes imply that adhesion/recognition molecules on cell surfaces provide information for specifying the positions that cells ultimately adopt.

(4) Origin-dependent cell adhesion

Grafting experiments within the pupal wing monolayer of *Manduca* have implied that differences in adhesive properties of epithelial cells exist along the proximodistal axis of the wing. These experiments have revealed

that the greater the distance separating host and graft cell populations along the proximodistal axis, the more circular and constricted the interface between graft and host cells.[18–20] These results demonstrate that the inferred adhesive properties of cells depend on their position and the differences in these adhesive properties of graft and host cells are a function of the distance between their original positions along the proximodistal axis of the wing.

(5) Short-range interaction mediated by cell adhesion proteins

The temporal and spatial patterns of distribution of two surface proteins have also been examined in the wing monolayers of developing adult *Manduca*. These two proteins are fasciclin II and neuroglian, both members of the immunoglobulin superfamily. Each protein has a well-defined pattern of expression, and each of the two cell types of the wing monolayer—GECs and SPCs—shows a unique pattern of expression during the period of cell rearrangement. As cells rearrange they differentially express these proteins on their lateral surfaces and basal processes; but before and after the rearrangement of cells, cells uniformly express neuroglian throughout the wing and express fasciclin II on only a small subset of wing cells.[7,9] The counterparts of these proteins in *Drosophila* are clearly involved in homophilic adhesive interactions when assayed following their expression in normally nonadhesive *Drosophila* S2 tissue culture cells.[21,22] Although neither fasciclin II nor neuroglian have been assayed for their ability to participate in heterophilic adhesive interactions, their vertebrate counterparts are known to participate in heterophilic interactions.[23,24] Heterophilic as well as homophilic interactions among the surface proteins expressed during cell rearrangement could provide a plethora of adhesive interactions that are instrumental in establishing the final scale patterns of lepidopteran wings.

3 A MODEL FOR PARALLEL ROW FORMATION OF SPCs WITH ORIGIN-DEPENDENT ADHESIVITY

Based on observations of row formation, we present a general model for cell rearrangement in which cells move up gradients of adhesivity. Since cells can apparently respond to non-adjacent neighbors during the time that they extend basal processes and contact cells that are several cell

diameters away, we use integrals to represent the local average adhesivity to which a cell responds.

3.1 Integral Representation

In this model we shall assume that there is only one cell type of importance (SPCs) and that two cells interact with each other according to the distance between their original locations as well as the distance between their current locations.

Let $n(\mathbf{x}, a, t)$ signify the cell density at position $\mathbf{x} = (x, y)$ at time t for the cells of a given adhesivity a that originate from a position that is a units of distance away from the body axis (the base of the wing). Suppose that cell movement is due to two processes, diffusion and convection (directed movement) in response to gradients of adhesivity. Due to the evidence for long-range interactions we shall consider a cell to respond to gradients in a spatially averaged adhesivity. As an evolution equation for cell density in space we write

$$n_t = D \nabla^2 n - \nabla \cdot [n\mathbf{c}], \tag{3.1}$$

where D is the diffusion coefficient. The convection velocity, $\mathbf{c}$, is given by

$$\mathbf{c} = C \nabla \left[\int\int\int n(\mathbf{x} - \mathbf{y}, a - s) w(\mathbf{y}, s)\, ds\, dy_1\, dy_2 \right], \tag{3.2}$$

where $\mathbf{x} = (x, y)$ and $\mathbf{y} = (y_1, y_2)$ are position variables, and C is a positive constant. The integral represents the spatially averaged adhesivity. The degree of adhesivity as a function of distance, $\mathbf{y}$, and adhesivity distance (distance in adhesivity space), s, are incorporated in the kernel $w(\mathbf{y}, s)$. For simplicity, we shall suppose that this is separable (i.e., that the effects of distance in physical and adhesivity space are independent of each other). We therefore write

$$w(\mathbf{y}, s) = g(\mathbf{y}) h(s). \tag{3.3}$$

We assume that g displays rotational symmetry in the two spatial dimensions, and h is symmetric in the adhesivity difference. We assume that there is a threshold in adhesivity marking a transition from attraction to repulsion. Also, the spatial kernel is such that very short range attraction is weaker than middle distance attraction. This reflects the fact that scale cells appear not to come into contact with one another during reorganization.

3.2 Mathematical Discussion of the Model and Numerical Simulation

Here we briefly study the mathematical model proposed above for describing the mechanisms underlying the spatial arrangement of SPCs in lepidopteran wings. Our goal is to investigate this model mathematically and numerically to test if it generates the parallel row pattern observed in the wing.

Using the assumption that $|\mathbf{y}| \ll 1$ and $|s| \ll 1$, we can simplify Eq. (3.1) by Taylor expanding Eq. (3.2):

$$n_t = D \nabla^2 n - C \nabla \cdot [n \nabla (n + \gamma \nabla^2 n + \beta n_{aa} + O(s^4 + |\mathbf{y}|^4)], \quad (3.4)$$

where

$$\beta = \frac{1}{2} \int s^2 h(s)\, ds, \quad (3.5)$$

$$\gamma = \frac{1}{2} \int\int y_1^2 g(\mathbf{y})\, dy_1\, dy_2. \quad (3.6)$$

The parameters β and γ are related directly to the effects of cell adhesion and distance, respectively.

This procedure reduces the integro-partial differential equation (3.1) to a partial differential equation and we carry out all our analyses on the latter. We consider the following two cases: origin-independent cell adhesion and origin-dependent cell adhesion.

Origin-independent cell adhesion We first consider a simple version of Eq. (3.4) in which we neglect the $O(s^4, |\mathbf{y}|^4)$ terms, and assume that $\beta \ll \gamma$, that is,

$$n_t = D \nabla^2 n - C \nabla \cdot [n \nabla (n + \gamma \nabla^2 n)]. \quad (3.7)$$

Hence, this version of the model ignores the effect of any origin-dependent cell adhesion mechanism. We impose periodic boundary conditions.

To determine the ultimate spatial patterns generated by the nonlinear model Eq. (3.7), we investigate the behavior of the amplitude functions in large time through a weakly nonlinear analysis. We use a singular perturbation technique to study the weakly nonlinear behavior of the amplitude functions in the vicinity of the primary bifurcation point. This analysis reveals that patterns of rows (stripes) and spots are possible. More precisely, if the uniform steady state is perturbed by a small initial random perturbation, then, depending on the parameter values, either a

stable striped spatial pattern or a stable spotted pattern will be generated eventually. However, we cannot determine the orientation of the striped pattern. In fact, stripes parallel or perpendicular to the body axis are equally likely (for full details, see Ref. 25).

Numerical simulation Here we numerically solve the model Eq. (3.7) by using a finite difference method with the aim of verifying our analytic predictions. The model parameters used in the numerical simulations are chosen to satisfy the conditions for generating spatial pattern (see Ref. 25, Table 1). We use a randomly distributed cell density as our initial condition and impose periodic boundary conditions. We choose the critical parameter values for C and D at the bifurcation point to be $C_c = 0.006$, $D_c = 0.09C_c$, and $\gamma = 0.0228$ which satisfy the condition for generating stripes. The numerical results obtained are shown in Figure 4, where the cell density distributions are shown at $t = 0$, $t = 2$, and $t = 40$. The lighter color represents higher cell density while the darker color represents lower cell density. The results clearly show that a striped pattern is generated by our model equation, in accordance with the results of our weakly nonlinear analysis (see Ref. 25, for a more detailed numerical study).

The effect of origin-dependent adhesivity The above study shows that the simple, origin-independent adhesivity model exhibits three possible arrangements of SPCs: rows, either parallel or perpendicular to the body axis, and spots. However, only rows parallel to the body axis are observed in the actual wing. Here we investigate the effect of including origin-dependent adhesivity in the model. With the origin-dependent adhesivity term the model equation becomes

$$n_t = D \nabla^2 n - C \nabla \cdot [n \nabla (n + \gamma \nabla^2 n + \beta n_{aa})]. \tag{3.8}$$

Note that $n(\mathbf{x}, a, t)$ is the cell density at position $\mathbf{x} = (x, y)$ at time t for the cells that originated a distance a away from the body axis. We assume that $n_{aa} = En_{xx}$, where E is a proportionality constant. The motivation for making this assumption is as follows: Note that the $\gamma \nabla^2 n = \gamma(n_{xx} + n_{yy})$ is a long range diffusion term. With the origin-dependent effect, cells are less likely to diffuse in the x-direction (i.e., perpendicular to the body axis), so βn_{aa} is acting as a negative diffusion term in the x-direction and reduces the net diffusion in the x-direction.

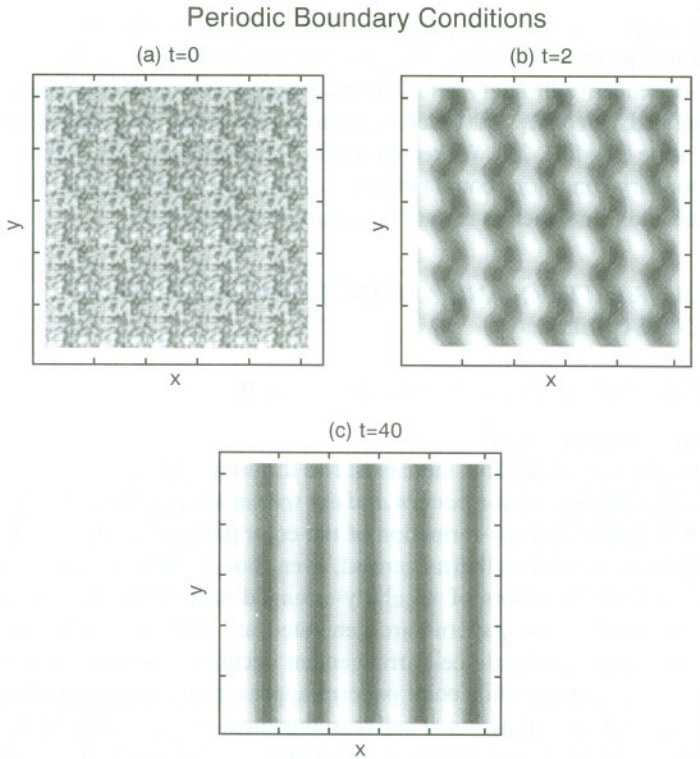

FIGURE 4 Results of simulation, where the cell density distributions are shown at (a) $t = 0$, (b) $t = 2$, and (c) $t = 40$. The lighter color represents high cell density while the darker color represents low cell density. We use a randomly distributed cell density as our initial condition and impose periodic boundary conditions. The critical parameter values for D and C at the bifurcation point are $C_c = 0.006$, $D_c = 0.09C_c$, and $\gamma = 0.0228$.

Therefore, Eq. (3.8) becomes

$$n_t = D \bigtriangledown^2 n - C \bigtriangledown \cdot [n \bigtriangledown (n + \gamma \bigtriangledown^2 n + \beta^* n_{xx})], \qquad (3.9)$$

where $\beta^* = E\beta$. Note that although β^* is negative, we assume that $\gamma + \beta^* \geq 0$, i.e., the effective diffusion in the x-direction is still positive.

When we add origin-dependent adhesion to the simple model Eq. (3.7), further nonlinear analysis shows that rows predominate in a larger region of parameter space. More importantly, the rows are predictably aligned,

that is, stripes can only lie parallel to the body axis under the effect of origin-dependent adhesivity. We also note that as long as the effect of origin-dependent adhesivity is sufficiently strong, spotted patterns cannot be generated. Our analysis is based on perturbations about a homogeneous steady state (see Ref. 25). We recognize that other factors such as initial and boundary conditions could potentially influence orientation of rows, but such additional factors are not necessary in this case.

4 COLOR PATTERN AND ARRANGEMENT PATTERN OF SCALE CELLS

4.1 Color Pattern Formation on Lepidopteran Wings

(1) Pattern formation mechanisms

As noted in the Introduction, there exist two different kinds of patterns in lepidopteran wings – *color pattern and the spatial arrangement of scale cells*. It is known that the formation of the color pattern is independent of the pattern of scale cell arrangement, even though the color patterns are formed by the colors of regularly-arranged scale cells. The time scales on which these patterns are generated are different from each other. The pattern of scale cell arrangement occurs in the early stages of adult development, while color patterns appear in later stages of adult development after completion of cell rearrangement.[1,26] In addition, the spatial scale of color pattern extends from tens to several hundreds of cell diameters, and no cell migration occurs during the period of color pattern determination. On the other hand, direct cell–cell interactions through filopodia during the period of cell rearrangement can only extend several cell diameters at most, which is very short relative to the scale of the color pattern (see Section 2 for details and Figure 3). Thus, a mechanism different from that proposed in Section 3 to account for the generation of scale spacing patterns is probably operating in the case of wing color patterns. Diffusion of small molecules through gap junctions is assumed to be a feasible mechanism for long distance cell-to-cell communication involved in forming color patterns.[1]

(2) Characteristics of color patterns

The color patterns on wings are species-specific, and they are often used for identification of species, while the arrangement of scale cells is not species-specific. Color patterns of dorsal and ventral monolayers

of wings are seldom alike in most Lepidoptera. They are also affected by the veins. However, due to the pioneering work of Schwanwitsch[27] and Süffert[28] on the ground plan for nymphalid butterfly color patterns, the complicated patterns on lepidopteran wings can be represented as a composite of a relatively small number of pattern elements. For example, (1) the symmetry system consists of color bands that run anterior to posterior across the wing; (2) the border ocelli system consists of a series of eyespots in the distal half of the wing; (3) the marginal bands are a pair of narrow bands near the wing's distal margin; (4) the dependent patterns are venous stripes, that is, a color pattern of the outline of the wing veins. This shows that the wing veins serve as the source of determination for this pattern element; (5) the ripple patterns run perpendicular to the proximodistal axis of the wing in a manner similar to the ripples in windblown sand.[29,1]

In spite of these simplifications, the problem of color pattern formation in wings is still not fully resolved. A few theoretical or mathematical models for color pattern formation have been proposed to account for specific features of the pattern, and we review these briefly in the next section.

4.2 Models for Color Pattern Formation

(1) Diffusion model

A simple model for the development of the commonly observed crossbands of pigmentation (see (2) in Section 4.1) shortly after pupation was proposed by Murray (see Ref. 29 or 30 and references therein). This model is based on a diffusing-morphogen-gene-activation system and extends the idea of a determination stream proposed by Kühn and von Engelhardt,[31] namely, that the anterior and posterior margins of the wing are sources from which there emanates a wave of morphogen concentration. Murray's model hypothesizes that the morphogen, concentration S, activates a gene product, concentration g, which, in turn, determines color pattern. The model, in non-dimensionalized form, is

$$S_t = \nabla^2 S - \gamma k S, \tag{4.10}$$

$$\frac{dg}{dt} = \gamma \left(k_1 S + \frac{k_2 g^2}{1 + g^2} - k_3 g \right), \tag{4.11}$$

where γ, k_1, k_2, k_3 and k are positive constants. The first equation models

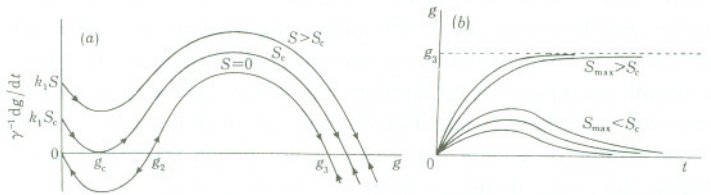

FIGURE 5 (a) Biochemical switch mechanism with typical bistable kinetics such as from Eq. (4.11). The graph shows $\gamma^{-1}\, dg/dt$ against g for appropriate k_1, k_2, k_3 and several values of S. The critical S_c is defined as having two stable steady states for $S < S_c$ and one, like $g = g_3$, for $S > S_c$. (b) Schematic behavior of g as a function of t from Eq. (4.11) for various pulses of S which increase from $S = 0$ to a maximum S_{max} and then decrease to $S = 0$ again. The lowest curve is for the pulse with the smallest S_{max}. The final state of g, for large time, changes discontinuously from $g = 0$ to $g = g_3$ if S_{max} passes through a critical threshold $S_{th} (> S_c)$ (from Ref. 29).

diffusion and linear degradation of S, where γ is a scaling parameter. The second equation models production and linear degradation of gene product. The interaction occurs via the activation of g by S. The kinetic parameters in the g equation are chosen so that the dynamics exhibit switch behavior (see Figure 5).

The equations are solved either on a sector of a circle, representing a wing, or a rectangle, representing a wing cell (i.e., the area of the wing delimited by two adjacent wing veins). The boundary conditions for S are a mixture of zero flux on some boundaries which are impermeable to S and fixed on other boundaries to represent sources of S.

Murray showed that this simple model could account for a wide variety of observed patterns. For example, it models patterns consistent with those observed after microcautery surgery. He also showed that for a given amount of S released, the width of the pattern on either side of the boundary is fixed for a given set of parameters. This is consistent with the observation of Schwanwitsch.[27] Varying the scale and geometry of the model wing leads to more complicated patterns that are consistent with those observed on certain butterfly and moth wings, while considering the model on a wing cell and varying the source strengths also leads to commonly observed patterns.

(2) Composite diffusion–lateral-inhibition model

Nijhout[32] presented a model for color patterns that incorporates the idea of sources and sinks of chemicals (extending the diffusion model

of 4.2.(1)), where the positions of the sources and sinks are determined by the concentration of an activator in a lateral inhibition reaction-diffusion model. He first presented a database of patterns occurring in the butterfly family Nymphalidae, that is, a catalogue of patterns that a realistic model must be able to reproduce. Experimental evidence suggests that color pattern formation is a two-step process: firstly, a spatial distribution of sources and sinks of pattern organizers is set up (during the larval stage). Secondly, these organizers induce colour patterning in their surroundings (completed during the early pupal stages). Nijhout solved the inverse problem, that is, he first investigated the distribution of sources and sinks that are sufficient to produce the required color patterns. Then, he used the lateral inhibition model of Meinhardt[33] to generate this distribution. The model has the form

$$a_t = \frac{ca^2}{h} - ak_a + D_a\left(a_{xx} + a_{yy}\right), \tag{4.12}$$

$$h_t = ca^2 - hk_h + D_h\left(h_{xx} + h_{yy}\right), \tag{4.13}$$

where a and h are the concentrations of activator and inhibitor, respectively, D_a, D_h, c, k_a and k_h are positive parameters. These equations model diffusion and linear degradation, with autocatalytic production of both a and h by the activator a, and inhibition of a production by the inhibitor h.

By imposing sources of activator on the boundaries, Nijhout showed that this model, for different values of boundary source strengths, D_a, D_h, k_a and k_h, can produce activator profiles which can determine the necessary distribution of sources for the second step of the color patterning process. As pointed out by Nijhout, the lateral inhibition model suffers from a sensitivity to parameter and scale changes that cannot be easily reconciled with experimental observation. Such sensitive behavior of reaction-diffusion models is well-known (see, for example, Ref. 34) and has been the subject of much theoretical study. It has been shown that appropriate modification of the diffusion coefficients can greatly increase the robustness of patterns to changes in scale,[35] while careful control of the boundary conditions can also enhance pattern robustness to changes in scale and parameter values.[36]

Several models have been proposed for spatial pattern formation in biology (for a review, see Murray 30, 1993). The vast majority of these models consist of coupled systems of partial differential equations, and they have been extensively studied and shown to exhibit a vast range of spatial patterns. In the first part of this paper, we considered spatial arrangement of scale cells in lepidopteran wings based on a number of key biological observations, and we developed a totally new model for pattern formation consisting of only one equation, of integro-partial differential type. We have shown that a simple version of this model can exhibit stripes or spots, but that a more complicated version can exhibit only stripes of a specific orientation that is consistent with biological observations. Single equation pattern formation models have also been developed in the mechanical theory of pattern formation (see Ref. 30 for a review of this theory) by Murray[37] and Zhu and Murray.[38]

One of the key questions in biological pattern formation is how does a particular pattern develop in a robust and reliable manner? For example, reaction-diffusion systems,[39] can exhibit spots or stripes on two-dimensional domains. It has been shown that the form of the nonlinearity is crucial in determining which of these patterns stabilizes.[40–43] More recently, Varea *et al.*[44] have shown that spatially varying parameters can be imposed to select the formation of stripes and control their orientation. In this paper, we have provided a novel mechanism (origin-dependent adhesivity) for selecting the formation of stripes over spots and orienting the stripes in the correct direction.

We have assumed that the arrangement of scale precursor cells in lepidopteran wings proceeds stepwise in time and that it consists of two different pattern forming processes, that is, uniform pattern formation of SPCs as the first step, noted in Section 2 (see also Figure 1(a)) and as the second step, the formation of parallel rows.[45] In relation to parallel row formation of scale cells, two other problems still remain, which we would like to note next. The first concerns the mechanisms that generate the uniform pattern of SPCs prior to parallel row formation. It has been suggested that the isotropic spacing pattern of SPCs can be generated through lateral inhibition—a type of cell–cell interaction whereby a cell that adopts a particular fate inhibits its immediate neighbors from doing likewise. The transmembrane proteins Notch and Delta (or their homologues) have been identified as mediators of the interaction—Notch

as receptor, Delta as its ligand on adjacent cells. Recently, a simple and general mathematical model of such contact-mediated lateral inhibition has been presented, based on the Delta–Notch mechanism of lateral inhibition.[46] In our numerical simulations in Section 3, we have not used a uniform pattern of SPCs as initial condition, but instead have imposed a randomly distributed cell density of SPCs. However, it should be noted that these random perturbations can be made extremely small without affecting the results of the simulations, and they reflect the fluctuations that one would expect in a biological system of this type. The second problem concerns cell proliferation during the rearrangement of cells. As noted in the Introduction, SPCs continue to differentiate from generalized epithelial cells during cell rearrangement. The increase in population of SPCs is around 20% of the total cell population. The exact value depends on the insect.[5,47] We have not included this in the model. It would result in a production term which would not affect the movement dynamics and would therefore have only a quantitative influence on the patterning behavior of the model; the main results of this paper would still hold.

Regarding color patterns of wings, it would be hard to construct a general model that could account simultaneously for all features of the patterns, because they involve several diverse pattern elements as noted briefly in Section 4.1. Some models have been presented based on diffusion and reaction-diffusion schemes. They are, however, all directed at modeling specific features in specific species that represent realistic replicas of such pattern elements as central symmetry system, eyespot morphogenesis, and intervenous stripes.[29,48] What we should develop next is a comprehensive model that can explain the causal basis of the patterning in any species of Lepidoptera.

In summary, the formation of color markings and the arrangement of scale cells in lepidopteran wings involve many general aspects of pattern formation including cell interactions operating on different temporal and spatial scales. The proposed models reflect this and lead to different types of systems of equations. In this paper we have tried to illustrate how these approaches are beginning to address some of the fascinating and fundamental problems concerning pattern formation in lepidopteran wings.

Acknowledgements

T.S. would like to thank Prof. H.F. Nijhout of Duke University for his suggestions and information on color patterns of butterfly wings. P.K.M. would like to thank the Facultad de Ciencias, Universidad Nacional Autonoma de Mexico for their hospitality. This work (JDM) was in part supported by grants from the U.S. National Science Foundation (DMS-9500766) and the U.S. National Institute of Health (2P41-RR01243-17).

TOSHIO SEKIMURA
College of Engineering, Chubu Univerisity
Kasugai, Aichi 487-8501, Japan

PHILIP K. MAINI
Centre for Mathematical Biology, Mathematical Institute,
University of Oxford, 24-29 St Giles', Oxford OX1 3LB, UK

JAMES B. NARDI
Department of Entomology, University of Illinois
320 Morrill Hall, 505 South Goodwin Avenue
Urbana, IL 61801, U.S.A.

MEI ZHU
Department of Mathematics, Pacific Lutheran University
Tacoma, WA 98447-0003, U.S.A.

JAMES D. MURRAY
Department of Applied Mathematics, University of Washington
P.O. Box 352420, Seattle, WA 98195-2420, U.S.A.

References

1. H.F. Nijhout, *The Development and Evolution of Butterfly Wing Patterns* (Smithonian Institution Press, Washington and London, 1991).
2. H. Ghiradella, *Microscopic Anatomy of Invertebrates* 11 A: Insecta (Wiley-Liss, Inc., 1998), pp. 257–287.
3. H.F. Nijhout, Dev. Biol. **80**, 275 (1980).
4. J.B. Nardi and S.M. Magee-Adams, Dev. Biol. **116**, 278 (1986).
5. A. Yoshida and K. Aoki, Develop. Growth Differ. **31**, 601 (1989).
6. A. Yoshida, Forma **5**, 65 (1990).
7. J.B. Nardi, Dev. Biol. **152**, 161 (1992).
8. L.I. Held, *Models for Embryonic Periodicity* (Karger, Basel, 1993).
9. J.B. Nardi, Dev. Dyn. **199**, 315 (1994).
10. P. Simpson, Development **109**, 509 (1990).
11. L.I. Held, Bioessays **13**, 633 (1991).
12. P. Heitzler and P. Simpson, Cell **64**, 1083 (1991).
13. S. Campuzano and J. Modolell, Trends Genetics **8**, 202 (1992).
14. C.Q. Doe and C.S. Goodman, Dev. Biol. **111**, 206 (1985).

15. J.A. Campos-Ortega, Trends Neurosci. **11**, 400 (1988).
16. H. Honda, M. Tanemura and A. Yoshida, Development **110**, 1349 (1990).
17. M. Locke and P. Huie, Nature **293**, 733 (1981).
18. J.B. Nardi and F.C. Kafatos, J. Embryol. Exp. Morphol. **36**, 469 (1976a).
19. J.B. Nardi and F.C. Kafatos, J. Embryol. Exp. Morphol. **36**, 489 (1976b).
20. J.B. Nardi, *Current Issues in Neural Regeneration Research* (ed. P.J. Reier) (New York: Alan R. Liss, 1988), pp. 127–136.
21. M. Hortsch, Y.E. Wang, Y. Marikar and A.J. Bieber, J. Biol. Chem. **270**, 18809 (1995).
22. G.M. Edelman and K.L. Crossin, Annu. Rev. Biochem. **60**, 155 (1991).
23. G. Kadmon, A. Kowitz, P. Altevogt and M. Schachner, J. Cell Biol. **110**, 193 (1990).
24. V.P. Mauro, L.A. Krushel, B.A. Cunningham and G.M. Edelman, J. Cell Biol. **119**, 191 (1992).
25. T. Sekimura, M. Zhu, J. Cook, P.K. Maini, and J.D. Murray, Bull. Math. Biol. (1998) (in press).
26. A. Yoshida, Spec. Bull. Lep. Soc. Jap. **6**, 447 (1988) (in Japanese).
27. B.N. Schwanwitsch, Proc. Zool. Soc. Lond. Ser B **34**, 509 (1924).
28. F. Süffert, Biologisches Zentralblatt **47**, 385 (1927).
29. J.D. Murray, Phil. Trans. R. Soc. Lond. B **295**, 473 (1981).
30. J.D. Murray, *Mathematical Biology* (Springer-Verlag, 1993).
31. A. Kühn and A. Engelhardt, Wilhelm Roux Arch. EntwMech, Org. **130**, 660 (1933).
32. H.F. Nijhout, Proc. R. Soc. Lond. B **239**, 81 (1990).
33. H. Meinhardt, *Models of Biological Pattern Formation* (Academic Press, New York, 1982).
34. J.B. Bard and I. Lauder, J. Theor. Biol. **45**, 501 (1974).
35. H.G. Othmer and E. Pate, Proc. Natn. Acad. Sci. U.S.A. **77**, 4180 (1980).
36. R. Dillon, P.K. Maini and H.G. Othmer, J. Math. Biol. **32**, 345 (1994).
37. J.D. Murray, In: Proc. 2nd Intl. Congress Industrial and Applied Maths. 1991, pp. 212–226. SIAM Publications: Philadelphia, 1992 [Plenary lecture].
38. M. Zhu and J.D. Murray, J. of Nonlinear Sci. **5**, 317 (1995a).
39. A.M. Turing, Phil. Trans. Roy. Soc. Lond. B **237**, 37 (1952).
40. B. Ermentrout, Proc. R. Soc. Lond. A. **434**, 413 (1991).
41. M.J. Lyons and L.G. Harrison, Dev. Dynamics **195**, 201 (1992).
42. B.N. Nagorcka and J.R. Mooney, IMA J. Math. Appl. Biol. & Med. **9**, 249 (1992).
43. M. Zhu and J.D. Murray, Int. J. of Bifurcation and Chaos **5** No.6, 1503 (1995b).
44. C. Varea, J.L. Aragón and R.A. Barrio, Phys. Rev. E **56**, No.1, 1250 (1997).
45. T. Sekimura and A. Yoshida, Forma **5**, 73 (1990).
46. J.R. Collier, N.A.M. Monk, P.K. Maini and J.H. Lewis, J. Theor. Biol. **183**, 429 (1996).
47. A. Yoshida, Forma **8**, No. 2, 203 (1993).
48. H.F. Nijhout, Scientific American **245**, 145 (1981).